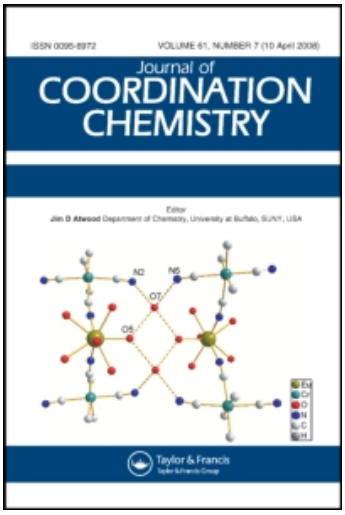

Journal of Coordination Chemistry
Publication details, including instructions for authors and subscription information:
http://www.informaworld.com/smpp/title~content=t713455674

Synthesis, crystal structure, and magnetism of a dinuclear nickel(II) complex $[Ni_2(MOBPT)_2(N_3)_4] \cdot 2H_2O$

Jie Yang[a]; Wei-Wei Bao[a]; Xiao-Ming Ren[b]; Yan Xu[a]; Xuan Shen[a]; Dun-Ru Zhu[a]
[a] College of Chemistry and Chemical Engineering, State Key Laboratory of Materials-oriented Chemical Engineering, Nanjing University of Technology, Nanjing, China [b] College of Science, Nanjing University of Technology, Nanjing, P. R. China

First published on: 29 July 2010

To cite this Article Yang, Jie , Bao, Wei-Wei , Ren, Xiao-Ming , Xu, Yan , Shen, Xuan and Zhu, Dun-Ru(2009) 'Synthesis, crystal structure, and magnetism of a dinuclear nickel(II) complex $[Ni_2(MOBPT)_2(N_3)_4] \cdot 2H_2O$', Journal of Coordination Chemistry, 62: 11, 1809 — 1816, First published on: 29 July 2010 (iFirst)
To link to this Article: DOI: 10.1080/00958970802709333
URL: http://dx.doi.org/10.1080/00958970802709333

Journal of Coordination Chemistry
Vol. 62, No. 11, 1 June 2009, 1809–1816

Taylor & Francis
Taylor & Francis Group

Synthesis, crystal structure, and magnetism of a dinuclear nickel(II) complex $[Ni_2(MOBPT)_2(N_3)_4]\cdot 2H_2O$

JIE YANG†, WEI-WEI BAO†, XIAO-MING REN‡, YAN XU†, XUAN SHEN† and DUN-RU ZHU*†

†College of Chemistry and Chemical Engineering, State Key Laboratory of Materials-oriented Chemical Engineering, Nanjing University of Technology, Nanjing, China
‡College of Science, Nanjing University of Technology, Nanjing, P. R. China

(*Received 6 July 2008; in final form 4 September 2008*)

A dinuclear nickel(II) complex, $[Ni_2(MOBPT)_2(N_3)_4]\cdot 2H_2O$ (MOBPT = 4-(*p*-methoxyphenyl)-3,5-*bis*(pyridine-2-yl)-1,2,4-triazole), has been synthesized and characterized by elemental analysis, UV, IR, ESI-MS, and single crystal X-ray crystallography. The complex crystallizes in triclinic system, space group $P\bar{1}$ with $a = 9.877(2)$ Å, $b = 10.396(2)$ Å, $c = 11.975(3)$ Å, $\alpha = 71.638(3)^\circ$, $\beta = 74.968(3)^\circ$, $\gamma = 64.747(3)^\circ$, $V = 1044.2(4)$ Å^3, $Z = 1$, $R = 0.0371$ for 5774 observed reflections. The crystal structure determination shows that the dinuclear Ni_2N_8 unit is almost planar with each Ni^{2+} coordinated by four nitrogens from two MOBPT ligands and two axial azides in a distorted octahedral geometry. Magnetic measurements reveal weak antiferromagnetic exchange in the complex.

Keywords: Crystal structure; Dinuclear complex; Triaryltriazole; Nickel(II); Magnetic property

1. Introduction

The coordination chemistry of triaryltriazoles and related ligands has attracted considerable attention [1] because of interesting magnetic properties [2–5] and structures [6, 7]. Iron(II) complexes with triaryltriazoles have spin-crossover properties which can be used as molecular electronics [8], memory devices [9], information storage [10], and switching materials [11]. Although major effort has focused on mononuclear complexes containing triaryltriazole ligands [12], dinuclear complexes have been rarely studied [13]. Recently, we synthesized the first dinuclear complex $[Ni_2(MOBPT)_2Cl_2(H_2O)_2]Cl_2\cdot 7H_2O$ with 4-(*p*-methoxyphenyl)-3,5-*bis*(pyridine-2-yl)-1,2,4-triazole (MOBPT), a triaryltriazole ligand [14]. As continuation of our investigation on the dinuclear complexes with triaryltriazoles, herein we present the synthesis, crystal structure and magnetism of a dinuclear nickel(II) complex with MOBPT, $[Ni_2(MOBPT)_2(N_3)_4]\cdot 2H_2O$ (**1**$\cdot 2H_2O$).

*Corresponding author. Email: zhudr@njut.edu.cn

Journal of Coordination Chemistry
ISSN 0095-8972 print/ISSN 1029-0389 online © 2009 Taylor & Francis
DOI: 10.1080/00958970802709333

2. Experimental

2.1. *Physical measurements*

All chemicals were of analytical grade. Solvents were purified by conventional methods. The ligand MOBPT was synthesized according to the literature method [15, 16]. Elemental analysis (C, H, N) was performed with a Thermo Finnigan Flash 1112A elemental analyzer. Electronic spectrum was obtained with a Perkin-Elmer Lambda 35 UV/VIS spectrometer in MeOH solution. IR spectrum was recorded on a Nicolet Avatar 380 FT-IR instrument (KBr discs) in the 4000–400 cm^{-1} region. Electrospray ionization mass spectrum (ESI-MS) was recorded on a Agilent 1100 LC/MSD SL spectrometer, with MeOH as the mobile phase; the flow rate of the mobile phase was 0.2 $cm^3\,min^{-1}$. The capillary voltage and temperature was 2500 V and 325°C, respectively. The flow of nebulizer gas and dry gas is 12 and 8 $cm^3\,min^{-1}$, respectively. Variable temperature magnetic susceptibilities of crystalline samples were measured on a Quantum Design MPMS SQUID-XL7 magnetometer. Diamagnetic corrections were made with Pascal's constants for all constituent atoms.

2.2. *Preparation of $[Ni_2(MOBPT)_2(N_3)_4]\cdot 2H_2O$*

To a colorless solution of MOBPT (198 mg, 0.6 mmol), in warm MeOH (40 cm^3), was added dropwise a grass green solution of $NiCl_2\cdot 6H_2O$ (143 mg, 0.6 mmol) in MeOH (5 cm^3). Then NaN_3 (156 mg, 2.4 mmol) was added. The resulting green solution was stirred at room temperature for 2 h. Evaporation of the solvent at room temperature for 4 weeks yielded green crystals suitable for X-ray diffraction. Yield based on MOBPT: 182 mg, 62%. Anal. Calcd for $C_{38}H_{34}N_{22}Ni_2O_4$ (%): C, 46.32; H, 3.34; N, 31.59. Found: C, 46.56; H, 3.50; N, 31.44. IR (KBr, cm^{-1}): 3371–3064 (m, b), 2041 vs, 1604 m, 1512 s, 1466 m, 1436 m, 1261 s, 1022 m, 845 m, 804 m, 643 m. ESI-MS: m/z 971.4; 758.2; 522.8; 358.1.

2.3. *X-ray crystallography*

A green block crystal of the complex, with dimensions $0.24\times 0.15\times 0.12\,mm^3$, was selected for lattice parameter determination and collection of intensity data at 293 K on a Brüker Smart APEX CCD diffractometer with monochromated Mo-Kα radiation ($\lambda = 0.71073$ Å) using a ϕ–ω scan mode. The data were corrected for Lorenz and polarization effects during data reduction. An empirical absorption correction based on ψ scans was applied. The structure was solved by direct methods and refined on F^2 by full-matrix least-squares methods using SHELXTL [17]. All nonhydrogen atoms were refined anisotropically. Hydrogens for C–H and O–H were placed in calculated positions and allowed to ride on the parent atoms to which they are attached. The contribution of these hydrogen atoms was included in the structure factor calculations. All computations were carried out using the SHELXTL program package. Analytical anomalous dispersion corrections were incorporated. The final R factor was 0.0371 $\{R_\omega = 0.0748$, $\omega = 1/[\sigma^2(F_o^2) + (0.04P)^2]$, $P=(F_o^2 + 2F_c^2)/3$ for 304 parameters, 2902 observed reflections $[I > 2\sigma(I)]\}$. The maximum and minimum residual peaks in the final differences maps were 0.442 and $-0.476\,e\,Å^{-3}$. Crystallographic data are summarized in table 1.

Table 1. Crystallographic data for $\mathbf{1} \cdot 2H_2O$.

Empirical formula	$C_{38}H_{34}N_{22}Ni_2O_4$
Formula weight	980.25
Crystal size (mm^3)	$0.24 \times 0.15 \times 0.12$
Crystal color	Green
Crystal system	Triclinic
Space group	$P\bar{1}$
Unit cell dimensions (Å, °)	
a	9.877(2)
b	10.396(2)
c	11.975(3)
α	71.638(3)
β	74.968(3)
γ	64.747(3)
Volume ($Å^3$)	1044.2(4)
Z	1
D_{Calcd} ($g\,cm^{-3}$)	1.559
$F(000)$	504
Temperature (K)	293(2)
Absorption coefficient (mm^{-1})	0.973
θ range (°)	1.81–26.0
Index range (h, k, l)	(−11/12, −12/12, −10/14)
Reflections collected	5774
Independent reflections	4040 ($R_{int} = 0.0417$)
Data/restraint/parameters	4040/3/304
Goodness-of-fit on F^2	1.003
Final R, $\omega R(I > 2\sigma(I))$	0.0371, 0.0748
R, ωR indices (all data)	0.0607, 0.1067
Largest difference peak and hole ($e\,Å^{-3}$)	0.442, −0.476

3. Results and discussion

The triaryltriazole ligand, MOBPT, reacts with $NiCl_2 \cdot 6H_2O$ and NaN_3 in 1 : 1 : 2 molar ratio to form a neutral dinuclear complex, $[Ni_2(MOBPT)_2(N_3)_4] \cdot 2H_2O$, which is stable in air. The elemental analysis is satisfactory and indicates that the complex contains two nickel atoms, two MOBPT ligands, four azide ions, and two water molecules. The MOBPT acts as doubly-bidentate chelating ligand in the complex [14].

3.1. *Crystal structure of $[Ni_2(MOBPT)_2(N_3)_4] \cdot 2H_2O$*

Single crystal X-ray analysis reveals that the complex contains a dinuclear neutral molecule as shown in figure 1. The complex contains $[Ni_2(MOBPT)_2(N_3)_4]$ and two water molecules. There is an inversion center at the center of $[Ni_2(MOBPT)_2(N_3)_4]$ making the two Ni atoms crystallographically equivalent in the solid state. The dinuclear $[Ni_2N_8]$ unit in $[Ni_2(MOBPT)_2(N_3)_4]$ is almost planar (mean deviation from the plane of 0.0337 Å). In this plane the dinuclear $(N1, N3, N4, N5)_2$ double-bridging coordination is observed in the $[Ni_2(MOBPT)_2(N_3)_4]$ molecule by two ligands. Each nickel is coordinated equatorially by four nitrogens from two MOBPT and two N_3^- axially, resulting in a distorted octahedral coordination environment. Selected bond lengths and angles are given in table 2. The Ni–N_{py} bond lengths [2.176(3)–2.227(3) Å]

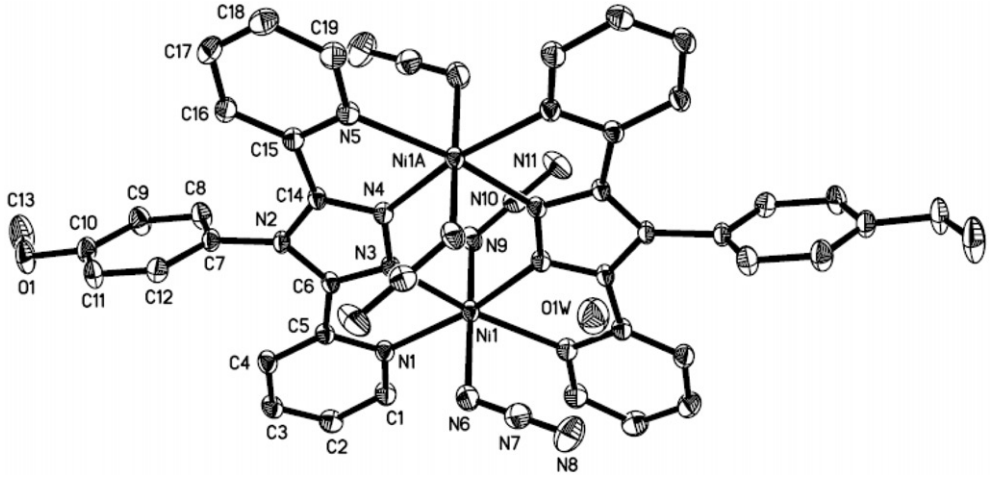

Figure 1. Projection of $\mathbf{1} \cdot 2H_2O$ with the atom labeling system. Hydrogen atoms are omitted for clarity.

Table 2. Selected bond distances (Å) and angles (°) for $\mathbf{1} \cdot 2H_2O$.

Bond lengths			
Ni(1)–N(1)	2.176(3)	Ni(1)–N(3)	2.050(3)
Ni(1)#1–N(4)	2.030(2)	Ni(1)#1–N(5)	2.227(3)
Ni(1)–N(6)	2.078(3)	Ni(1)–N(9)	2.087(3)
N(4)–C(14)	1.306(4)	N(1)–C(5)	1.357(4)
N(3)–C(6)	1.311(4)	N(5)–C(15)	1.360(4)
N(3)–N(4)	1.355(3)	O(1)–C(10)	1.360(4)
N(2)–C(7)	1.464(4)	O(1)–C(13)	1.431(5)
N(6)–N(7)	1.189(4)	N(7)–N(8)	1.170(4)
N(9)–N(10)	1.192(4)	Ni(1)–Ni(1)#1	4.169(5)
Bond angles			
N(3)–Ni(1)–N(4)#1	92.57(10)	N(1)–Ni(1)–N(5)#1	115.82(10)
N(1)–Ni(1)–N(3)	76.46(10)	N(6)–Ni(1)–N(1)	86.37(12)
N(6)–Ni(1)–N(3)	92.67(12)	N(6)–Ni(1)–N(5)#1	85.45(12)
N(6)–Ni(1)–N(4)#1	95.24(12)	N(9)–Ni(1)–N(4)#1	91.51(11)
N(9)–Ni(1)–N(3)	92.14(11)	N(9)–Ni(1)–N(1)	87.98(11)
N(9)–Ni(1)–N(5)#1	91.34(11)	N(9)–Ni(1)–N(6)	171.53(12)
N(3)–Ni(1)–N(5)#1	167.35(10)	N(1)–Ni(1)–N(4)#1	168.99(10)
N(6)–N(7)–N(8)	179.3(4)	N(9)–N(10)–N(11)	179.6(4)

Note: Symmetry code: 1: $1-x$, $1-y$, $-z$.

are longer than the Ni–N_{trz} bond lengths [2.030(2)–2.050(3) Å] and both somewhat larger than the corresponding bond lengths observed in the related dinuclear nickel(II) complexes: $[Ni_2(MOBPT)_2Cl_2(H_2O)_2]Cl_2 \cdot 7H_2O$ [14] [2.159(4)–2.192(3) Å; 2.038(3)–2.044(3) Å, respectively], $[Ni_2(NH_2BPT)_2Cl_2(H_2O)_2]Cl_2 \cdot 4H_2O$ [6] [2.155(1)–2.164(1) Å; 2.013(1)–2.029(1) Å] and $[Ni_2(ibdpt)_2(MeCN)_4](ClO_4)_4$ [5] [2.139(3)–2.149(3) Å; 2.023(3)–2.031(3) Å]. The Ni–N_{azide} bond lengths [2.078(1)–2.087(3) Å] are shorter than those [2.100(3)–2.111(2) Å] observed in the monodentate azide complexes $[Ni(N_3)_2(bte)_2]_n$ and $[Ni(N_3)_2(bbtz)_2]_n$ [18]. The azide is linear [bond angles N6–N7–N8 and N9–N10–N11 are 179.3(4)° and 179.6(4)°, respectively] as usual for monodentate azide complexes. The Ni–Ni distance in the present complex is 4.169(5) Å,

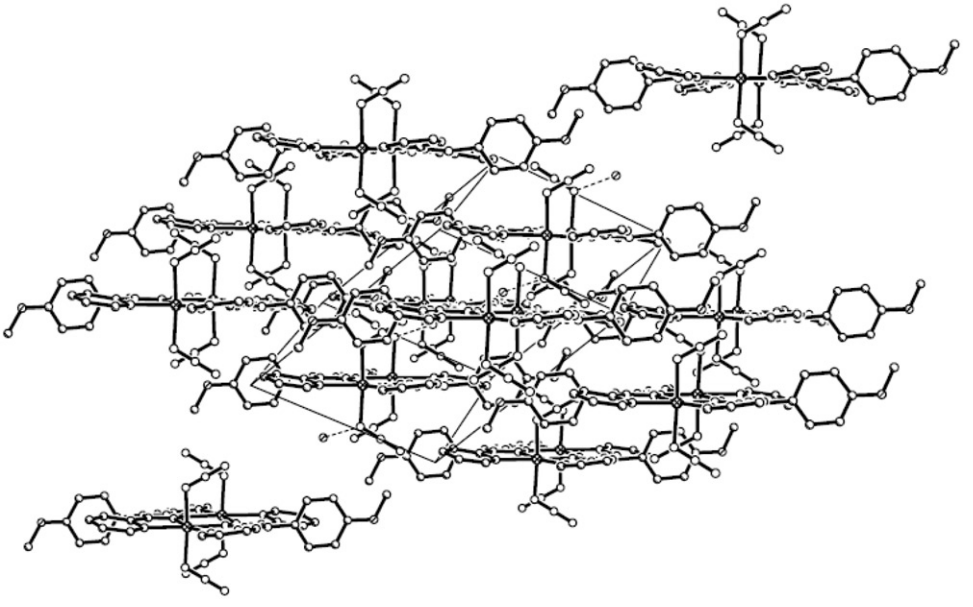

Figure 2. The unit cell packing of $\mathbf{1} \cdot 2H_2O$. Broken lines indicate hydrogen bonds.

slightly smaller than that found in $[Ni_2(MOBPT)_2Cl_2(H_2O)_2]Cl_2 \cdot 7H_2O$ [4.189(5) Å] and slightly larger than found in related dinuclear nickel(II) complexes: $[[Ni_2(NH_2BPT)_2Cl_2(H_2O)_2]Cl_2 \cdot 4H_2O$ [4.1348(3) Å] and $[Ni_2(ibdpt)_2(MeCN)_4](ClO_4)_4$ [4.1107(9) Å]. The triazole ring makes dihedral angles of 11.4(1)° and 9.2(1)° with the N1- and N5-containing pyridine rings, respectively, while the phenyl ring is inclined relative to the triazole ring by an angle of 75.1(1)°. The crystal structure is further stabilized by intermolecular O–H $\cdots$ N hydrogen bonds [O(1W) $\cdots$ N(8) = 2.983(1) Å, O(1W)–H(1WA) $\cdots$ N(8) = 177.9(1)°; O(1W) $\cdots$ N(9) = 2.924(1) Å, O(1W)–H(1WB) $\cdots$ N(9) = 169.9(1)°] (figure 2). These hydrogen bonds make the two N_3^- groups in the axial positions be *syn* relative to the N6–Ni1–N9 linkage.

3.2. *IR spectrum*

In the IR spectrum of $\mathbf{1} \cdot 2H_2O$, a very strong band at 2041 cm^{-1} is assigned to N_3^- stretch. There are several broad, medium bands at *ca.* 3371 and 3064 cm^{-1}, attributed to H–O–H stretching vibrations, suggesting the existence of hydrogen bonding interactions [19]. This is in agreement with the X-ray analysis. The IR spectrum of the complex can also be closely related to that of free MOBPT. One of the most diagnostic changes occurs between 1610 and 1560 cm^{-1}; free MOBPT shows a strong band at 1584.5 cm^{-1} and a medium band at 1567.3 cm^{-1}, attributable to the pyridine ring vibrations. Upon pyridine coordination to a metal, the higher band is shifted by *ca.* 15 wavenumbers. Thus, in the spectrum of the complex, a band at 1604 cm^{-1} (m) can be assigned to the coordinated pyridine ring [20]. This means that in $\mathbf{1} \cdot 2H_2O$, MOBPT ligand uses two pyridine nitrogens and two triazole nitrogens for doubly-bidentate binding (N1, N3, N4, N5), as confirmed by the structure determination. In addition,

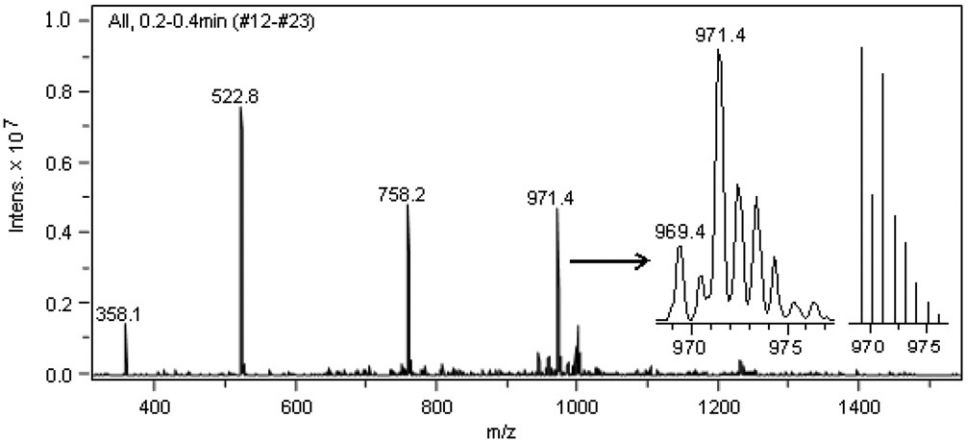

Figure 3. ESI-MS of $\mathbf{1}\cdot 2H_2O$ in methanol. The insets show the experimental and calculated isotopic patterns of the *m*/*z* 971.4 peak.

two bands at 1261 (s) and 1022 cm^{-1} (m) are due to Ar–O–C asymmetric and symmetric stretches, respectively. The C–H out-of-plane absorption of the *para*-substituted phenyl is at 845 (m) and 804 cm^{-1} (m). The triazole out-of-plane ring absorption is observed at 643 cm^{-1} (m).

3.3. *ESI-MS spectrum*

The structure of $\mathbf{1}\cdot 2H_2O$ in solution was also studied by ESI-MS [21]. Figure 3 displays a positive ion ESI mass spectrum of the complex in methanol, where four main peaks were observed. The major peak at *m*/*z* 971.4 with mass separation *m*/*z* 1 clearly confirms the +1 charge of $[Ni_2(MOBPT)_2(N_3)_3]^+$ $2H_2O\cdot CH_3OH$. The experimental isotopic patterns were in agreement with the calculated ones. The other peaks at *m*/*z* 758.2, 522.8, and 358.1 could be assigned to $[Ni(MOBPT)_2(N_3)]^+$; $[\mathbf{1}\cdot 2H_2O + 2H]^{2+}\cdot 2CH_3OH$; and $[Ni(MOBPT)_2]^{2+}$, respectively. The results indicate the presence of complicated equilibria in the matrix solution. Comparison of the ESI-MS peak intensities among the species clearly show the presence of the relatively abundant $[Ni_2(MOBPT)_2(N_3)_3]^+$ species, which has been isolated and characterized by X-ray crystallography.

3.4. *Magnetic property*

The variable-temperature magnetic susceptibility of $\mathbf{1}\cdot 2H_2O$ performed on a crystalline sample using a SQUID magnetometer in the temperature range 1.8–300 K within an applied field of 2000 Oe is shown in figure 4 in the form of a χ_m *versus* *T* plot. The temperature dependence of the χ_m data reveals the existence of weak antiferromagnetic coupling between the Ni(II) sites joined *via* the μ-N^3, N^4 triazole ligand. The χ_m value at 300 K is 0.0079 emu mol^{-1}, which is expected for a pair of uncoupled octahedrally coordinated Ni(II) ions with $^3A_2$ ground state. As the temperature is decreased, χ_m gradually increases to 0.0822 emu mol^{-1} at 18 K and then

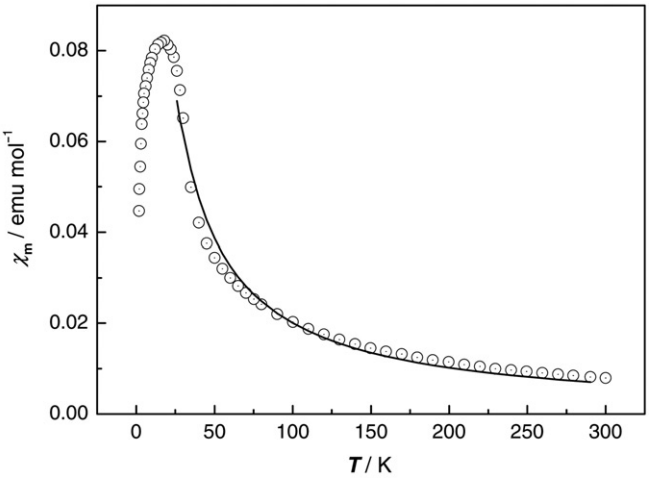

Figure 4. χ_m (○) *vs.* T plot for $[Ni_2(MOBPT)_2(N_3)_4]\cdot 2H_2O$.

decreases to 0.045 emu mol^{-1} at 1.8 K. The magnetic data can be fitted to an $S=1$ Heisenberg dimer – $2JS_1S_2$ model, equation (1) [22], where N is Avogadro's number, k is the BM and β is the Boltzmann constant; g, J, and zj' are adjustable parameters. The best least squares fit from 28 to 300 K gave $g=2.04$, $J=-2.1(7)\,cm^{-1}$, $zj'=0.03(1)\,cm^{-1}$. The coupling constant J is less than that observed in $[Ni_2(MOBPT)_2Cl_2(H_2O)_2]Cl_2\cdot 7H_2O$ [14].

$$\chi_m=\frac{\chi_d}{1-(2zj'/Ng^2\beta^2)\chi_d} \qquad \chi_d=\frac{2Ng^2\beta^2}{kT}\times\frac{e^{2J/kT}+5e^{6J/kT}}{1+3e^{2J/kT}+5e^{6J/kT}} \tag{1}$$

3.5. *Electronic absorption spectrum*

In the UV spectrum of $\mathbf{1}\cdot 2H_2O$ in methanol solution, two intense bands at 239 and 294 nm are attributed to the MOBPT π–π^* and n–π^* transitions (228.5 and 274.5 nm for free MOBPT–methanol solution). In addition, there is a weak peak at 384 nm for $\mathbf{1}\cdot 2H_2O$, which corresponds to d–d transitions for high spin Ni(II) in the pseudo-octahedral environment [16], in agreement with the results of magnetic measurement.

Supplementary material

Crystallographic data for the structure reported in this article has been deposited with the Cambridge Crystallographic Data Center as supplementary publication No. CCDC-693045. Copies of this information may be obtained free of charge via http://www.ccdc.cam.ac.uk (or from the Cambridge Crystallographic Centre, 12 Union Road, Cambridge CB2 1EZ, UK; Fax: +44-1223-336033; E-mail: deposit@ccdc.cam.ac.uk).

Acknowledgments

This work was funded by the National Nature Science Foundation of China (No. 20771059, 20771050) and the Natural Science Foundation of Jiangsu Province (BK2008371).

References

[1] (a) M.H. Klingele, S. Brooker. *Coord. Chem. Rev.*, **241**, 119 (2003); (b) P.J. van Koningsbruggen. *Top. Curr. Chem.*, **233**, 123 (2004); (c) J.A. Kitchen, S. Brooker. *Coord. Chem. Rev.*, **252**, 2072 (2008).
[2] R. Prins, P.J.M.L. Birker, J.G. Haasnoot, G.C. Verschoor, J. Reedijk. *Inorg. Chem.*, **24**, 4128 (1985).
[3] W.M.E. Koomen-van Oudennie, R.A.G. de Graaff, J.G. Haasnoot, R. Prins, J. Reedijk. *Inorg. Chem.*, **28**, 1128 (1989).
[4] M.H. Klingele, B. Moubaraki, K.S. Murray, S. Brooker. *Chem. Eur. J.*, **11**, 6962 (2005).
[5] M.H. Klingele, P.D.W. Boyd, B. Moubaraki, K.S. Murray, S. Brooker. *Eur. J. Inorg. Chem.*, 910 (2005).
[6] F.S. Keij, R.A.G. de Graaff, J.G. Haasnoot, J. Reedijk. *J. Chem. Soc., Dalton Trans.*, 2093 (1984).
[7] P.J. van Koningsbruggen, D. Gatteschi, R.A.G. de Graaff, J.G. Haasnoot, J. Reedijk, C. Zanchini. *Inorg. Chem.*, **34**, 5175 (1995).
[8] J. Kröber, E. Codjovi, O. Kahn, F. Groliere, C. Jay. *J. Am. Chem. Soc.*, **115**, 9810 (1993).
[9] O. Kahn. *Chem. Britain*, **FEBRUARY**, 24 (1999) [Magazine: Olivier Kahn, Chemistry in Britain, FEBRUARY, 24–27 (1999)].
[10] O. Kahn, C.J. Martinez. *Science*, **279**, 44 (1998).
[11] D. Zhu, Y. Xu, Z. Yu, Z.J. Guo, H. Sang, T. Liu, X.Z. You. *Chem. Mater.*, **14**, 838 (2002).
[12] (a) D. Zhu, Y. Song, Y. Xu, Y. Zhang, H.K. Fun, X.Z. You. *Polyhedron*, **19**, 2019 (2000); (b) D.R. Zhu, T.W. Wang, S.L. Zhong, X. Yan, X.Z. You. *Chin. J. Inorg. Chem.*, **20**, 508 (2004); (c) D.R. Zhu, Z.X. Wang, J. Song, Y.Z. Li, D.Y. Lan. *Chin. J. Inorg. Chem.*, **21**, 128 (2005); (d) L. Qi, D. Zhu, D.J. Xie, Y.F. Wu, X. Shen. *Chin. J. Inorg. Chem.*, **24**, 868 (2008).
[13] (a) S.K. Mandal, H.J. Clase, J.N. Bridson, S. Ray. *Inorg. Chim. Acta*, **209**, 1 (1993); (b) S.C. Shao, Z.L. You, S.P. Zhang, H.L. Zhu, S.W. Ng. *Acta Crystallogr.*, **E61**, m265 (2005); (c) M.H. Klingele, P.D.W. Boyd, B. Moubaraki, K.S. Murray, S. Brooker. *Eur. J. Inorg. Chem.*, 573 (2006).
[14] J. Zhou, J. Yang, L. Qi, X. Shen, D. Zhu, X. Yan, Y. Song. *Transition Met. Chem.*, **32**, 711 (2007).
[15] H.K. Fun, K. Chinnakali, S. Shao, D. Zhu, X. You. *Acta Crystallogr.*, **C55**, 770 (1999).
[16] (a) D. Zhu, Y. Song, Y. Liu, Y. Xu, Y. Zhang, X. You. *Transition Met. Chem.*, **25**, 589 (2000); (b) D. Zhu, Y. Xu, Y. Mei, Y. Shi, C. Tu, X. You. *J. Mol. Struct.*, **559**, 119 (2001).
[17] G.M. Sheldrick. *SHELXTL, Structure Determination Software Programs*, Bruker Analytical X-ray Systems Inc, Wisconsin, USA (1997), Version 5.10.
[18] (a) X. Zhu, Y.M. Zhang, B.L. Li, Y. Zhang. *J. Coord. Chem.*, **59**, 513 (2006); (b) L.Y. Wang, Y.F. Peng, Y.P. Zhang, B.L. Li, Y. Zhang. *Acta Crystallogr.*, **C63**, 2m297 (2007).
[19] K. Nakamoto. *Infrared Spectra of Inorganic and Coordination Compounds*, p. 166, Wiley, New York (1970).
[20] U. Hartmann, H. Vahrenkamp. *Inorg. Chim. Acta*, **239**, 13 (1995).
[21] S.R. Wilson, A. Yasmin, Y. Wu. *J. Org. Chem.*, **57**, 6941 (1992).
[22] A.P. Ginsberg, R.L. Martin, R.W. Brookes, R.C. Sherwood. *Inorg. Chem.*, **11**, 2884 (1972).